# Scanning-tunneling-microscopy observation of stress-driven surface diffusion due to localized strain fields of misfit dislocations in heteroepitaxy

G. Springholz and G. Bauer
*Institut für Halbleiterphysik, Johannes Kepler Universität Linz, 4040 Linz, Austria*

V. Holy
*Department of Solid State Physics, Masaryk University, Brno 61137, Czech Republic*
(Received 20 May 1996)

Using *in situ* scanning-tunneling microscopy, the influence of localized strain fields of misfit dislocations on epitaxial growth is studied. We observe pronounced surface deformations caused by single dislocations and *dislocation reactions*, in excellent quantitative agreement with calculations based on elasticity theory. Due to the local reduction of strain energy at the surface above the interfacial dislocations, ridgelike structures are formed due to stress-driven surface diffusion during growth. [S0163-1829(96)07132-9]

Strained-layer heteroepitaxy has attracted tremendous interest in the last few years, since it allows more degrees of freedom in design and fabrication of modulated semiconductor heterostructures. However, practical applications of such structures require not only a tight control of defect density but also of surface morphology during growth. With respect to the latter, recent experimental and theoretical work has revealed that the presence of *strain* results in a fundamentally different evolution of surface morphology as compared to unstrained films.[1–8] This is because, on one hand, any lateral variation of strain on the surface leads to local differences in the growth rate and thus to the formation of surface corrugations, on the other hand, that surface corrugations allow an *elastic* relaxation of strain energy due to the additional free surfaces.[1–6] As a consequence, a spontaneous transition from two-dimensional (2D) to three-dimensional (3D) growth (Stranski-Krastanov growth mode) often occurs.

While this strain-induced growth mode instability is now quite well understood, the situation is much less clear in the case of relaxation by misfit dislocations. Although it has been known for a long time that misfit dislocation formation is accompanied by significant changes in surface morphology, a most prominent example being the ''crosshatch'' surface pattern,[9,10] its origin has remained a controversial issue. While some groups found evidence for stress-driven surface diffusion due to dislocation strain fields,[11–15] recent work has shown that the crosshatch pattern formation is dominated by slip steps created by the glissile motion of dislocations during the relaxation process,[10,16,17] a mechanism which in fact has been proposed already in the early work of Matthews and Blakeslee.[9]

In the present work, we have developed a technique for *in situ* study of the localized strain fields of misfit dislocations based on scanning-tunneling microscopy (STM). It is shown that in STM images pronounced surface deformations are observed due to strong lattice distortions around the subsurface dislocations,[17–19] which can be described quantitatively by taking into account the relaxation of the free surface. The resulting *strain contrast* in the STM images is used for an analysis of misfit dislocation reactions in which dislocations with different orientations of the Burgers vector are produced. Since by STM it is thus possible to image *simultaneously* the localized surface strain fields of interfacial dislocations, as well as the atomic scale surface features produced by epitaxial growth, we are able to present unambiguous experimental evidence for lateral mass transport driven by the localized strain fields of misfit dislocations. However, a systematic analysis shows that for the usual heteroepitaxial growth conditions this effect is overwhelmed by the surface modifications due to the slip steps associated with misfit dislocation formation.

In the following, we study molecular-beam epitaxy of EuTe on PbTe(111), a material system used for the study of the magnetic interactions in low dimensions.[20] Both compounds crystallize in the rocksalt crystal structure, and their lattice mismatch is 2.06%. Since EuTe usually grows in a Stranski-Krastanov growth mode on PbTe(111), rather low substrate temperatures ($<280\,^{\circ}$C) are used in order to maintain a 2D layer-by-layer growth mode.[7] In our experiments, first, several-$\mu$m-thick, fully relaxed PbTe buffer layers are deposited on $BaF_2(111)$, serving as ''virtual substrates.'' In the second step, EuTe is deposited up to layer thicknesses slightly above the critical layer thickness in order to initiate the formation of misfit dislocations. Then, after rapid cooling, the samples are transferred to an attached UHV STM chamber for imaging of the surface structure.

The surfaces of the PbTe buffer layers are extremely smooth, and consist of large growth spirals formed around the core of threading dislocations.[21] Initially, this surface structure is replicated on the EuTe surface due to the layer-by-layer growth mode. At the critical layer thickness $h_c$ of 15 monolayers (ML), however, totally straight surface step lines of several $\mu$m in length are formed on the surface. This results from the glide of grown-in threading dislocations parallel to the surface, as described by the classical Matthews-Blakeslee model.[9] In this glide process, the dislocations bend over at the layer-substrate interface, and strain-relaxing misfit dislocation (MD) segments are formed. Thus each glide step on the surface corresponds to a MD segment at the heterointerface. In our materials system, the Burgers vector **b** is usually of $\frac{1}{2}[110]$ type, and glide first takes place in the primary (100)[011] glide system. This yields pure edge-type

 

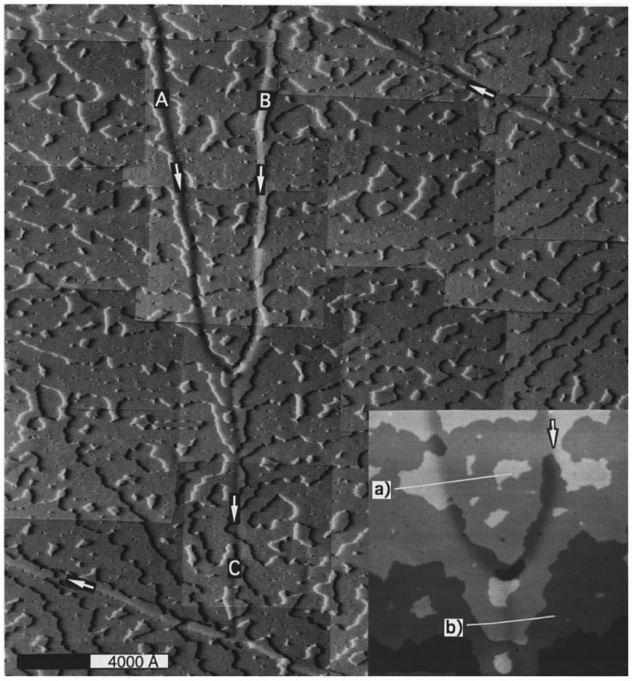


FIG. 1. STM image of an annealed 25-ML EuTe layer on PbTe(111). The gray scale corresponds to the local derivative of height in the horizontal direction. The inset shows the actual height image of the center part, and the surface profiles along lines (a) and (b) are shown in Fig. 2. The arrows indicate misfit dislocations formed by the strain relaxation process.

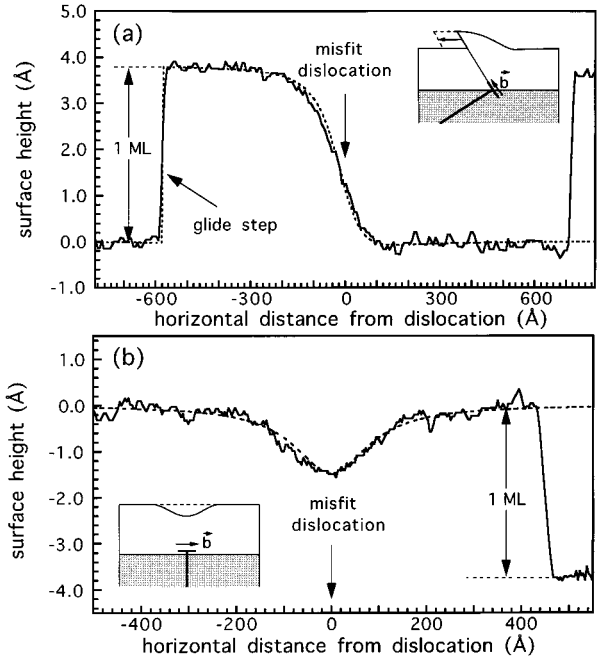


FIG. 2. Full lines: STM surface profiles measured across the misfit dislocations marked by lines (a) and (c) in Fig. 1. Dashed lines: calculated surface profiles.

MD's along the $\langle \overline{1}10 \rangle$ glide directions. At larger layer thicknesses, due to high excess stresses, secondary glide systems are activated, and then misfit dislocations along other directions are also observed.[21]

While the totally straight glide steps are the most striking surface features produced by the strain relaxation process, taking a closer look one finds that in the vicinity of these glide steps an additional long-range deformation is superimposed on the surface. This is shown in Fig. 1, where the STM image of an annealed 25-ML EuTe layer on PbTe(111) is depicted, with the gray scale corresponding to the local derivative of the height in the horizontal direction. In this representation, broad dark (or light) lines appear on the surface (see arrows), corresponding to surface areas where the local slope of the surface deviates from the horizontal direction. Since along each of these lines a glide step is also present on the surface, they are related to misfit dislocations at the EuTe/PbTe interface. Clearly, the strain fields of the interfacial dislocations extend all the way up to the surface, causing a *local bending* of the surface lattice planes. Therefore, the dislocation contrast in the derivative STM images is very similar to that in bright field transmission electron microscopy. As shown in the actual STM surface profile across one of the dark lines [Fig. 2(a)], a *wavelike* surface deformation is observed above the misfit dislocation. It is constant all along the MD line and has an amplitude equal to the monolayer thickness (3.8 Å).

In the center part of Fig. 1, the two MD's marked by *A* and *B* bend over to form a new single dislocation. As shown in the inset of Fig. 1 (the actual height image of this surface area), the wavelike surface deformation for *A* and *B* are opposite in direction, i.e., the surface is bent downwards for dislocation *A* and upwards for dislocation *B*, which corresponds to a dark (light) line in the derivative STM image. Thus the $\frac{1}{2}[110]$-type Burgers vectors of the dislocations must have a different orientation with respect to the interface. Assuming $\mathbf{b}=\frac{1}{2}[110]$ for *A* and $\frac{1}{2}[\underline{10}\underline{1}]$ for *B*, a dislocation reaction according to $\frac{1}{2}[110]+\frac{1}{2}[\underline{10}\underline{1}]=\frac{1}{2}[011]$ takes place, yielding a dislocation with a Burgers vector now oriented *parallel* to the interface. Indeed, the surface deformation observed above dislocation *C* has a completely different character, i.e., instead of a wavelike deformation only a shallow surface *depression* is formed [Fig. 2(b)]. Energetically, this type of dislocation reaction is very factorable, since the dislocation energy is reduced by a factor of 2 whereas the in-plane component of **b** is essentially preserved, which means that the *same* amount of in-plane strain is relieved by the single dislocation *C* as for dislocations *A* and *B* together.

For the theoretical description of the surface deformations and local strain fields induced by the interfacial misfit dislocations, we use isotropic elasticity theory, neglecting the rather small differences in the elastic constants of EuTe and PbTe. In order to take into account the relaxation of the free surface, we apply the method of image dislocations as described in Ref. 22. Since for edge dislocations this is still not sufficient to satisfy the boundary condition of a traction-free surface, additional fictive stresses have to be taken into account in order to cancel the surface shear stresses as well. From our calculations it turns out that the type of surface deformation indeed depends strongly on he orientation of the Burgers vector. For the usual MDs with **b** of $\frac{1}{2}[110]$ type, the calculations yield a wavelike surface deformation with an amplitude exactly equal to the normal component of **b**. In fact, the comparison with the STM data [Fig. 2(a)], which was calibrated by the 3.81-Å height of the monolayer steps

on the surface, shows an excellent agreement between measured and calculated surface profiles (full and dashed lines, respectively), without using any fit parameters. For dislocations with **b** parallel to the interface (e.g., dislocation *C* in Fig. 1), the calculations yield a shallow surface depression, which is again in excellent quantitative agreement with the experimental data [see Fig. 2(b)].

Since the local lattice deformations induced by MDs are directly visible by STM, the question arises of how these local strain fields influence epitaxial growth. In general, the evolution of the surface morphology is governed by nonuniformities in the surface chemical potential $u(x)$, which in the case of stressed surfaces is given by[4]

$$u(x)=u_0+\gamma\Omega\kappa(x)+\Omega w(x), \tag{1}$$

where $u_0$ represents the chemical potential of the unstressed flat surface, $\gamma$ the surface free energy per unit area, $\Omega$ the volume of the EuTe atom pair, $\kappa(x)$ the surface curvature, and $w(x)$ the local strain energy density on the surface. Changes in the surface morphology are then produced by diffusive flux of atoms along the surface, driven by the *gradients* in the surface chemical potential.[4] If we consider the situation of a reasonably flat ($\kappa=0$), biaxially stressed layer (homogeneous misfit strain $\varepsilon_0$) with a single dislocation parallel to $z$ at $y=d$ below the surface, then, initially, this mass transport is determined only by the gradients of the strain energy $w$ caused by the *localized* strain field $\hat{\varepsilon}_{ij}$ of the dislocation. Since $\varepsilon_0$, $w$ depends only on the horizontal distance $x$ from the dislocation:

$$w(x)=M\left(\varepsilon_0^2+\varepsilon_0\hat{\varepsilon}_{xx}(x)+\frac{\hat{\varepsilon}_{xx}^2(x)}{2+2\nu}\right)+2\mu\hat{\varepsilon}_{xz}^2(x). \tag{2}$$

Here $M=2\mu(1+\nu)/(1-\nu)$, $\mu$ and $\nu$ are the shear modulus and Poisson ratio, and $\hat{\varepsilon}_{xx}(x)$ and $\hat{\varepsilon}_{xz}(x)$ are tensor components of the dislocation strain field, determined from the calculations described above. It is noted that the last term in Eq. (2) is nonzero only for MDs with screw component. For pure edge dislocations, the variation of the strain energy $w$ is directly proportional to the variation of $\hat{\varepsilon}_{xx}(x)$ in a first-order approximation. Thus the diffusive flux along the surface is proportional to the *gradients* of $\hat{\varepsilon}_{xx}(x)$ times the mobility of the surface adatoms (surface diffusion length).

Figure 3 shows the variation of the surface strain $\varepsilon_{xx}$ as a function of the lateral distance $x$ from the dislocation for EuTe layers with thicknesses of $d=15$, 30, and 60 ML, and for the two possible orientations of **b**. $\varepsilon_0=2.06\%$ is the background misfit strain due to the PbTe buffer layer. It turns out that the dislocation strain fields are localized within a lateral distance equal to the layer thickness, and that at the critical layer thickness (15 ML) almost *all* of the misfit strain normal to the dislocation is locally relaxed, i.e., at the minimum of $\varepsilon_{xx}(x)$ the strain energy is reduced by a factor of 2. For the two orientations *A* and *C* of **b** this corresponds to a local reduction of the chemical potential of 9 or 7 meV, respectively, per EuTe atom pair. This should have a notable influence on the evolution of surface morphology, and the formation of ridgelike surface structures would be expected during growth.

Experimentally, however, for the usual MDs with **b** of $\frac{1}{2}[110]$ type, actually no such surface features are observed in our STM images (Fig. 4, black arrows). For this, several reasons exist. First of all, since for EuTe growth very low substrate temperatures have to be used in order to suppress the 3D Stranski-Krastanov growth mode, lateral mass transport is strongly limited by the very short adatom surface diffusion lengths of about 200 Å.[24] Second, for the tilted orientation of **b** the reduction of strain on one side of the MD

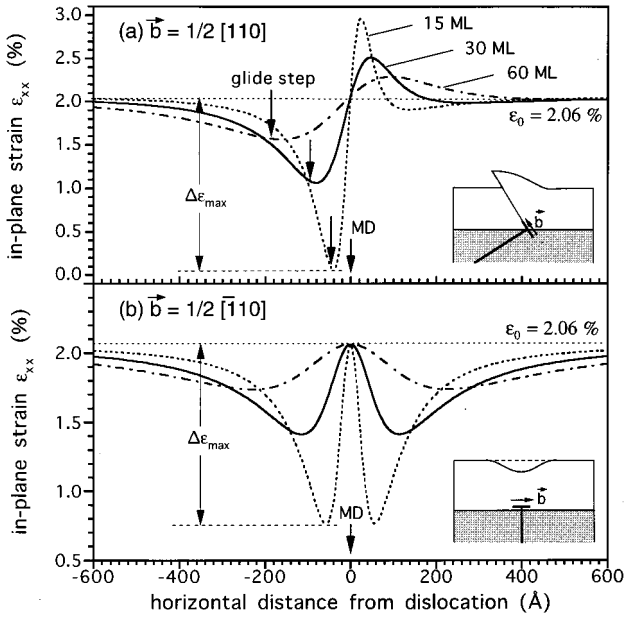


FIG. 3. Variation of the in-plane strain $\varepsilon_{xx}$ on the surface due to the localized strain field $\hat{\varepsilon}_{xx}(x)$ of a misfit dislocation with (a) $\mathbf{b}=\frac{1}{2}[110]$ and (b) $\mathbf{b}=\frac{1}{2}[011]$ and for EuTe layer thicknesses of 15, 30, and 60 ML (dashed, full, and dash-dotted lines, respectively). $\varepsilon_0=2.06\%$ is the misfit strain due to the PbTe buffer layer.

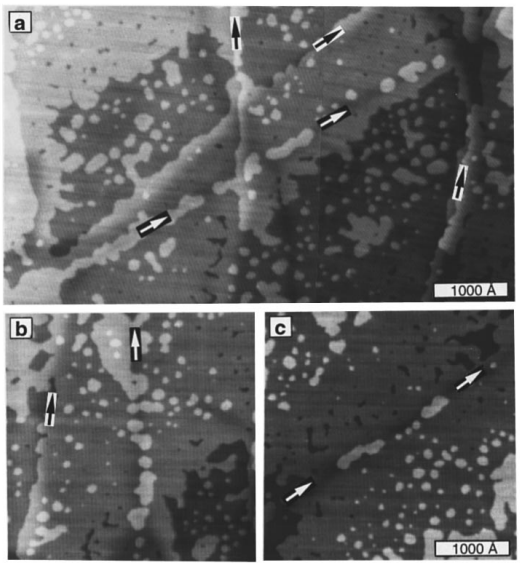


FIG. 4. STM height images of a quenched 30-ML EuTe layer on PbTe(111) showing preferential adatom incorporation at surface sites above misfit dislocations with **b** of $\frac{1}{2}[0\bar{1}1]$ type (dark lines marked by white arrows). For the regular $\frac{1}{2}[110]$-type misfit dislocations (lines where the contrast changes gradually from dark to light, marked by black arrows), no such effect is observed.

is accompanied by a strain increase on the opposite side [see Fig. 3(a)]. Thus additional adatom flux can be attracted only from one side of the MD, whereas flux from the opposite side is blocked by an energetic barrier. Finally, the surface glide step associated with the $\frac{1}{2}[110]$-type MDs coincides almost exactly with the local minimum of the surface strain energy [see Fig. 3(a)]. Since this glide step is a very effective sink for the free surface adatoms, instead of nucleating a surface ridge, the attracted adatom flux actually leads only to an enhanced growth rate at the glide step, or, in other words, to an increase of the step propagation velocity. Only after the glide steps have grown far away from the spatially fixed dislocation strain fields may the formation of additional surface features be expected.

The situation is completely different for MD's with **b** parallel to the interface. In this case (1) no glide step is produced on the surface, and (2) the misfit strain is reduced everywhere in the vicinity of the dislocation [see Fig. 3(b)]. As shown in Fig. 4, for these dislocations we *indeed* observe preferential nucleation of monolayer islands and the formation of ridgelike surface structures self-aligned to the interfacial dislocations, which are visible as dark lines in the STM images (white arrows). This is clear evidence of net mass transport to the local minimum of strain energy associated with these dislocations. However, this does not trigger the nucleation of 3D islands as in Stranski-Krastanov growth, since by the local reduction of strain energy the driving force for 3D islanding is also removed.

In spite of this clear evidence of the existence of stress-driven mass transport due to the localized strain fields of MD's, this effect cannot always be assumed to be the origin of the morphological changes observed in strained-layer heteroepitaxy. There are several reasons for this: First, MD's are usually formed by dislocation glide within slip planes inclined to the interface. As discussed above, these types of MD's are not very effective for stress-driven surface diffusion, but even more importantly, the large number of associated glide steps already drastically changes the surface morphology.[16,17,21] On the other hand, the more effective dislocations with **b** parallel to the interface are only rarely produced in heteroepitaxy. Second, as shown in Fig. 3, the dislocation strain fields decay rapidly with increasing layer thickness, and at the same time more and more misfit strain is relaxed. Due to the both effects [see Eq. (2)], the variations of strain energy and thus the influence of MD's on diffusive mass transport on the surface decreases drastically as epitaxial growth proceeds.

As a consequence the most pronounced effects of dislocations would be expected for heteroepitaxy of *highly* mismatched systems when the misfit dislocations are initially located very close to the epitaxial surface due to the small critical layer thickness. However, there a crossover to a completely different strain relaxation mechanism (coherent islanding) takes place, and then the effect of misfit dislocations is completely screened by the surface roughness resulting from the 2D to 3D growth-mode transition, which occurs long before the first MD is formed. Although usually this growth mode transition can be suppressed by freezing of the surface adatom mobility during growth, then lateral mass transport due to the dislocation strain fields is also very limited.

In conclusion, it was shown that localized strain fields of misfit dislocations induce significant surface deformations, which produce a strong *strain contrast* in the STM images. The shape of the surface deformations is found to depend strongly on the *orientation* of the Burgers vector, which is in excellent quantitative agreement with calculations based on the elasticity theory. This not only allows us to observe and analyze *dislocation reactions by in situ* STM, but also to correlate *directly* atomic scale epitaxial surface features with the strain fields of misfit dislocations extending from the interface up to the epitaxial surface. Our calculations show that at the critical layer thickness about *half* of the total strain energy is locally relieved by misfit dislocations, and due to stress-driven surface diffusion preferential epitaxial growth is observed at surface sites above dislocations.

Work supported by ÖNB GME, and BMWVK, Vienna, Austria.

[1] D. J. Eaglesham and M. Cerullo, Phys. Rev. Lett. **64**, 1943 (1990).
[2] S. Guha *et al.*, Appl. Phys. Lett. **57**, 2110 (1990).
[3] C. W. Snyder *et al.*, Phys. Rev. Lett. **66**, 3032 (1991).
[4] D. J. Srolovitz, Acta Metallogr. **37**, 621 (1989).
[5] J. Tersoff and F. K. LeGoues, Phys. Rev. Lett. **72**, 3570 (1994).
[6] C. Ratsch and A. Zangwill, Surf. Sci. **293**, 123 (1993).
[7] G. Springholz and G. Bauer, Phys. Rev. B **48**, 10 998 (1993).
[8] D. E. Jesson *et al.*, Phys. Rev. Lett. B **48**, 10 998 (1993).
[9] J. W. Matthews and A. E. Blakeslee, J. Cryst. Growth **27**, 118 (1974).
[10] K. H. Chang *et al.*, J. Appl. Phys. **67**, 4093 (1990).
[11] W. T. Pike *et al.*, J. Vac. Sci. Technol. B **10**, 1990 (1992).
[12] E. A. Fitzgerald *et al.*, J. Vac. Sci. Technol. B **10**, 807 (1992).
[13] X. C. Zhou *et al.*, in *Common Themes and Mechanisms of Epitaxial Growth*, edited by P. Fuoss, J. Tsao, D. W. Kisker, A. Zangwill, and T. F. Kuech, MRS Symposia Proceeding No. 312 (Materials Research Society, Pittsburgh, 1993), p. 77.
[14] L. B. Freund, G. E. Beltz, and F. Jonsdotttir, in *Thin Films: Stresses and Mechanical Properties IV*, edited by P. H. Townsend, J. P. Weins, J. Sanchez, Jr., and P. Bøgeson, MRS Symposia Proceeding No. 308 (Materials Research Society, Pittsburgh, 1993), p. 383.
[15] A. G. Cullis *et al.*, J. Cryst. Growth **158**, 15 (1996).
[16] S. Y. Shirayev *et al.*, Appl. Phys. Lett. **64**, 3305 (1994).
[17] M. A. Lutz *et al.*, Appl. Phys. Lett. **64**, 3305 (1994).
[18] R. Stalder *et al.*, Appl. Phys. Lett. **59**, 1960 (1991).
[19] G. Springholz and G. Bauer, Appl. Surf. Sci. (to be published).
[20] J. J. Chen, G. Dresselhaus, M. S. Dresselhaus, G. Springholz, C. Pichler, and G. Bauer, Phys. Rev. B (to be published).
[21] N. Frank *et al.*, Phys. Rev. Lett. **73**, 2236 (1994).
[22] P. Hirth and J. Lothe, *Theory of Dislocations* (Wiley, New York, 1972).